The quartz resonator: Electrochemical applications

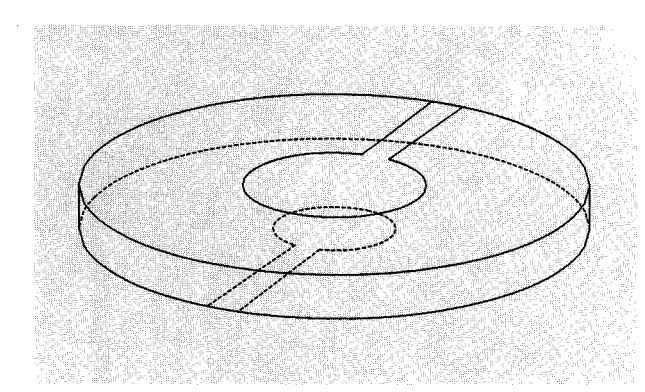
by K. K. Kanazawa O. R. Melroy

Since the discovery that the oscillations of resonating quartz crystals can be sustained in a liquid environment, such crystals have quickly found use as a sensitive microbalance in electrochemistry, making possible in situ measurements of mass changes at the electrochemical interface. The early contributions of the IBM Almaden Research Center to this exciting field of development are sketched. The principles of operation are detailed, with emphasis on an intuitive description to permit considerations of new applications. Mass density changes of the order of 10 nanograms per square centimeter (ng/cm²) are routinely detectable as changes in the resonant frequency of about a hertz. The mass density of a monolayer of material ranges from a few tens of ng/cm² for polymeric materials to a few hundreds of ng/cm² for metals. Detailed analysis of the electrical behavior of the resonator in liquid media shows that the resonant frequency, the quality factor of the resonance, and the admittance at resonance are all sensitive to the viscoelastic properties of the contacting liquid, having implications in the study of the behavior of non-Newtonian fluids, including polymeric films.

Introduction

The piezoelectric quartz resonator has been used since the 1960s for monitoring film deposition and growth in vacuum deposition systems. A general discussion of the properties of quartz crystals as used in resonators can be found in the review by Brice [1]. The resonator consists of a particular cut of a single crystal of quartz (the AT cut is popular for these applications) and takes the form of a flat circular disk having metallized electrodes on the two opposing surfaces, as shown in Figure 1. The electrodes are typically gold or platinum layers of the order of a few thousand Å in thickness. In its most common implementation, this electromechanical resonator is used as the frequencydetermining element of an electronic oscillator, and the changes in the oscillation frequency are recorded. The resonant frequency is generally of the order of several MHz. Mass uptake or removal on the electrode surface is reflected by a change in its resonant frequency. This relationship was first quantified by Sauerbrey [2], showing that the frequency decreased linearly with mass uptake. Subsequent studies have shown the validity of this relationship for thin metallic films; with increasing film thickness, however, important deviations were found. Additional studies extended the thickness range [3-6]. The identification of the key source for the failure of the linear relationship as the elastic behavior of the overlying film was made by Miller and Bolef [7]. A useful formulation of this model was presented by Lu and Lewis [8], who

*Copyright 1993 by International Business Machines Corporation. Copying in printed form for private use is permitted without payment of royalty provided that (1) each reproduction is done without alteration and (2) the *Journal* reference and IBM copyright notice are included on the first page. The title and abstract, but no other portions, of this paper may be copied or distributed royalty free without further permission by computer-based and other information-service systems. Permission to republish any other portion of this paper must be obtained from the Editor.



Sketch of a typical quartz transducer used as a resonator for gravimetric measurements. The electrodes are paddle-shaped and are shown with unequal radii. Associated shear motions occur in the plane of the disk in a direction chosen to be along the direction of the handle of the paddles.

developed a concise expression for the frequency change including the elastic properties of the film.

During the late 1970s, the quartz microbalance provided a key measurement capability as a film deposition monitor. Several investigators had considered the use of the resonator in liquid media, but had discarded the idea on the grounds that liquids would completely dampen the mechanical resonance. In 1980, Nomura [9] constructed a microbalance system and showed that despite the conceptual objections, the oscillations of the quartz resonator could be maintained in a liquid. He has since used improved versions of the systems for a great variety of analytical measurements [10–13]. Also reported in 1980 was the use of such resonators as detectors in liquid chromatography [14]. These accomplishments spurred the continually increasing use of the microbalance for studies in electrochemical environments.

To most successfully use the properties of the resonator in a liquid environment and to expand its range of applications requires a fairly detailed understanding of its behavior in such an environment. An intuitive description of the behavior is given, not only to provide a useful basis for working with the resonator, but also to give a more concrete meaning to the mathematical descriptions to follow. It is assumed that use is made of AT-cut quartz crystals. The direction normal to the planar faces of the disk is assumed to be the z direction. As indicated in Figure 1, the two electrodes are assumed to be of unequal areas. An electrical potential across the piezoelectric quartz crystal creates a shear strain parallel to an x axis which lies in the planar face. If the potential is made alternating, bulk shear waves propagating in the z direction are excited. These waves reflect from the upper and lower surfaces. At certain critical frequencies of excitation, the

waves interfere constructively, giving rise to electromechanical resonances. Values for the quality factor, or Q, of these resonances (the ratio of the resonant frequency to the full width in frequency at half the maximum amplitude of the conductance) are quite high. Typical values for the resonators in our laboratory routinely run in the range of many tens of thousands. At these resonances, standing sinusoidal shear waves are created in the bulk of the quartz having antinodes (points of maximum amplitude) at the exposed surfaces. Considerations of symmetry show that for the symmetrically loaded quartz resonator, only the fundamental and its odd harmonics can be excited. The shear motions on the upper and lower surfaces are in opposite directions. The amplitude of the shear vibration depends upon the applied potential and the quality factor of the resonator, but can be calculated to be as small as angstroms with voltages of the order of a volt. Despite the small amplitude of this vibration, the forces applied to a film deposited on the surface of the resonator (and vice versa) are very large, being proportional to the acceleration, which increases as the square of the applied frequency. The forces acting on such an overlying film amount to tens of thousands of g. The large acceleration of the surface is the source of the extraordinary mass sensitivity of the microbalance.

As previously mentioned, the free surfaces of the resonator are antinodes of vibration; this property gives rise to an important simplification. The acoustic shear waves generated in the quartz crystal are coupled to any overlying film, of course. But in the case of a "thin" film having thickness negligible compared to the wavelength of the coupled shear wave, it is essentially unstrained because the film lies in an antinodal region. Its effect on the resonant frequency of the resonator is then independent of its acoustical properties and dependent only on its mass density. This is the basis for the linear relation between the mass density and frequency change, as expressed by Sauerbrey. The difference between the initial unloaded frequency $f_{\rm U}$ and the frequency when loaded with the film $f_{\rm L}$ is $\Delta f = f_{\rm U} - f_{\rm L}$, and is given by

$$\Delta f = -\frac{2f_0^2}{\sqrt{\rho_0 \mu_0}} m', \tag{1}$$

where f_0 is the resonant frequency of the unloaded resonator, m' is the mass density, $\rho_{\rm Q}$ is the density of the quartz crystal, and $\mu_{\rm Q}$ is its elastic shear modulus. With the sensitivity as described by Equation (1), applications were quickly extended from the vacuum environment to analytical chemical areas [15, 16]. As the film thickness increases, an increasing fraction of the shear wave occupies the film, and the quartz with its overlayer must be considered as a compound resonator. The shear waves reflect not only from the free surfaces of the quartz and

the overlying film, but also from the interfacial boundary. The influence of a finite film thickness was studied in some detail by Miller and Bolef [7] for elastic (loss-free) films and was cast in an elegant form by Lu and Lewis [8]. It was found that the simple linear relationship of Sauerbrey was valid up to frequency changes of about 2%; beyond that region a closed analytical expression was obtained which included not only the density of the film but its elastic shear modulus as well.

If the film is not perfectly elastic, but also exhibits viscosity, the resulting frictional dissipation absorbs energy from the waves. Losses in the film profoundly change the behavior of the resonator. The statement that "liquids cannot support a shear wave" is common and underlies the earlier belief that the acoustic shear waves coupled from a resonator into an interfacing liquid would suffer such large losses that the resonance would be lost. The work of Nomura, showing the continued oscillation of the quartz resonator in liquid, prompted a reexamination of this matter; it was shown that the losses incurred by coupling the shear wave into the liquid were limited by the very fact that shear waves are not supported in the liquid. The amplitude of the coupled shear waves decreases exponentially with distance, and the finite depth of penetration limits the loss. The frequency of the resonator is, however, decreased because of the additional mass, and the losses of the resonator are substantially increased, reflecting the viscous slippage of the shear waves in the liquid. Theoretical calculations for a typical 5-MHz resonator with a Q of 1.3×10^5 predict a frequency decrease by 700 hertz and a drop in Q to 3.5×10^3 if one of its faces is exposed to water. In practice, one often finds that the observed frequency decrease is larger than this value. This has been ascribed to the roughness of the surface, entraining some liquid in surface "pockets" and causing an additional frequency decrease because of the mass of the trapped liquid.

The quartz surface at the liquid interface is very close to being an antinode for liquids which are Newtonian, e.g., most common solvents. The principal effect of the liquid is a decrease in the ${\cal Q}$ of the resonator and an additional constant offset in its resonant frequency. The sensitivity to deposited mass remains unchanged.

The foregoing qualitative discussion was intended to provide an intuitive understanding of the operation of the quartz resonator. A more quantitative treatment is required to provide quantitative analysis of experimental data, to provide predictive capabilities for new applications, and to provide a means of assessing sensitivity to possible interfering mechanisms.

Quantitative description

The fundamental equations and boundary conditions which are invoked to derive quantitative relations for the

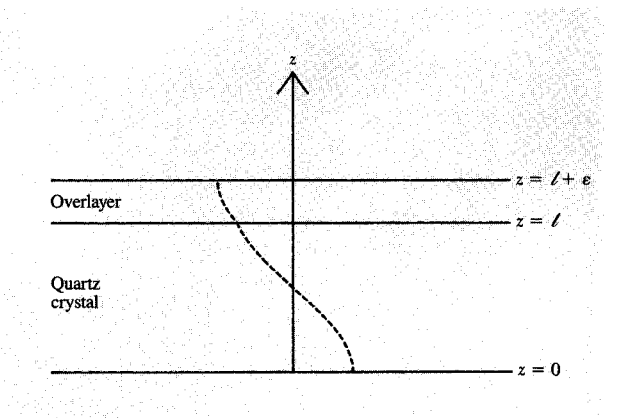


Figure 2 Geometry assumed for compound resonator analysis. Shear displacement during resonance is indicated by the dotted line.

resonating system not only provide a clear view of the approximations made, but also direct attention to those aspects of implementation of the technique to which particular care must be given. For these reasons, the mathematical descriptions are sketched in the following section, which is not prerequisite for an initial general reading of the applications, but provides a basis for a more in-depth approach.

The quartz resonator coupled to an overlayer forms a two-layer compound resonator in the general case. This two-layer structure is sketched in Figure 2. The origin of the z axis (z = 0) is assumed to lie in the plane of the lower free surface of the quartz; the thickness of the quartz is designated as ℓ , and the thickness of the overlying film is designated as ε . The dashed line designates the transverse shear amplitude, u(z, t). Two methods of proceeding under these guidelines are possible. In what we call the "mechanical model," the electrical properties of the quartz are not specifically included, and the problem is treated purely as the mechanical resonance induced by the constructive interference of the shear waves in the quartz crystal and the overlayer. The piezoelectric property of the crystal can be included in a somewhat ad hoc manner, knowing that the principal effect of its piezoelectric property on its mechanical shear motion is to make it appear to have a larger shear modulus. An effective "stiffened" value is used to describe the shear modulus in the stress-strain relation for the crystal. This simplified mechanical model has the virtue that an analytical expression can be obtained for the resonant frequency. The solution, however, describes only the resonant frequency.

A more general, "complete" solution can be obtained by specifically including the electrical properties of the

quartz crystal and the attendant electrical boundary conditions. A complete solution to the problem was first given by Benes [17] and applied to the important problem of the harmonic behavior of resonators with elastic overlayers. An alternate physically based approach was taken by Reed et al. [18], who specifically treated the case of the viscoelastically loaded resonator. This type of treatment obtains as a solution the electrical admittance of the compound resonator at arbitrary frequencies. From the admittance, both the resonant (series) and antiresonant (parallel) frequencies can be determined for the fundamental resonance as well as for the harmonics. In addition, other parameters such as the resonant Q and the resonant resistance can also be determined. This ability to determine the effect of the overlayer's mechanical properties on several measurable resonator parameters suggests that admittance studies, or, equivalently, impedance studies of these resonators have the potential for providing additional information concerning overlayer effects.

• Mechanical model

The results of such an analysis have been briefly described earlier [19], but the physical basis that underlies it was not included. Here we trace the development of the analysis, starting with the general mechanical stress-strain relation

$$\Pi = \mu \frac{\partial u(z, t)}{\partial z} + \eta \frac{\partial v(z, t)}{\partial t}, \qquad (2)$$

where Π is the shear force applied to the material in N/m², μ is the elastic shear modulus in N/m², u(z, t) is the spatial displacement in shear of the material on the plane zat time t in meters, η is the shear viscosity of the material in N·s/m², and v(z, t) is the velocity of the spatial displacement, viz., $v(z, t) = \partial u(z, t)/\partial t$ in m/s. The strains are assumed to be linearly dependent on the stress, and the viscosity of the quartz is assumed to be zero. When Equation (2) is used to describe the quartz, μ takes on the effective value of the shear modulus μ_0 = 2.947 × 10¹⁰ N/m². This value for the effective shear modulus is obtained from the value for the so-called frequency constant of 1670 kHz·mm given in Sauerbrey's original paper [2]. It is assumed that the quartz crystal is essentially lossless. When Equation (2) is used to describe the overlayer, the values for the overlayer, μ_{L} and η_{L} , are used. The relation can be used for pure Newtonian liquids where $\mu_{\rm r} = 0$ or for the general viscoelastic material.

In addition to the stress-strain relations for the two materials, it is also necessary to use Newton's second law via the net force per unit area applied to a slab of material of thickness dz; thus,

$$\frac{\partial \Pi}{\partial z} dz = \rho dz \frac{\partial v(z, t)}{\partial t}.$$
 (3)

The stress-strain relations, coupled with Newton's law, are sufficient to show that in the harmonic approximation, where we restrict our attention to variables which are varying as $e^{j\omega t}$, the solutions for the displacement u(z,t) take the form of shear waves traversing the media, undamped in the case of quartz where the viscosity had been assumed to be zero, and strongly damped in the case of Newtonian liquids. The relations take the general form

$$u(z,t) = [\tilde{U}_{\perp}e^{-(jk+\alpha)z} + \tilde{U}_{\perp}e^{+(jk+\alpha)z}]e^{j\omega t}, \tag{4}$$

where \overline{U}_+ and \overline{U}_- are the wave amplitudes traveling in the +z and -z directions, respectively, k is the propagation constant for the shear wave, and α is its decay constant. Precise forms for k and α are given in the Appendix. They are both functions of the density of the medium and its shear modulus and viscosity. For the overlayer, α tends toward zero as the viscosity decreases, vanishing for $\eta=0$.

To find the resonant frequencies, however, it is necessary to invoke the mechanical boundary conditions which must be satisfied. The two free surfaces, the uncoated face of the quartz crystal and the free surface of the overlayer, are presumed to be unconstrained. That is, no stress is assumed to be applied to these surfaces. Defining the free surface of the quartz to be at z=0 and that of the overlayer to be at $z=\ell+\varepsilon$, on those two planes, $\Pi=0$. At the interface between the quartz and the overlayer located at $z=\ell$, the following conditions apply: First, the stress across the interface must be continuous, namely

$$\Pi^{\text{Qtz}}(\ell) = \Pi^{\text{Film}}(\ell). \tag{5}$$

Finally, the so-called "no-slip" condition is assumed to apply; that is, the displacement across the interface is assumed to be continuous. Thus,

$$u^{\text{Qtz}}(\ell) = u^{\text{Film}}(\ell). \tag{6}$$

By requiring that the waves in the media meet these boundary conditions, one is led to an equation in complex variables which must be satisfied. Both the real part and the imaginary part cannot be simultaneously satisfied. In a simplified approach (referred to as the "mechanical model" approach), it is assumed that the solution corresponds to satisfying the real part of this equation. This leads to a frequency described by

$$-\omega\sqrt{\rho_{Q}\mu_{Q}}\tan\left(\pi\frac{\Delta\omega}{\omega_{0}}\right)$$

$$=(\mu\alpha-\omega k\eta)\frac{1-e^{-4\alpha\varepsilon}}{1+e^{-4\alpha\varepsilon}+2e^{-4\alpha\varepsilon}\cos 2k\varepsilon}$$

$$+(\mu k+\omega\alpha\eta)\frac{2e^{-2\alpha\varepsilon}\sin 2k\varepsilon}{1+e^{-4\alpha\varepsilon}+2e^{-2\alpha\varepsilon}\cos 2k\varepsilon}.$$
(7)

Here, ω_0 is the initial unloaded frequency of the resonator and $\Delta\omega$ is the frequency change with respect to that unloaded frequency. The assumed satisfaction of only the real part of this equation is a crucial approximation in this model, but comparisons with the results from a more complete model, to be described next, show excellent agreement. It is felt that this is a consequence of the fact that the Q value of the compound resonator continues to be high, even when the overlayer is a liquid.

• Complete model

By using a more rigorous model (referred to as the "complete model"), the result is obtained in the form of the electrical admittance of the compound resonator as a function of the applied frequency. As stated earlier, a sinusoidally varying electrical potential applied across the electrodes of the quartz portion of the compound resonator is assumed to generate shear waves in the quartz which are then coupled into any overlayer. At particular frequencies, the shear waves will interfere constructively, giving rise to the resonances. An electrical current is also induced by the rf voltage, and the phase and magnitude of this current relative to the exciting voltage e_{r} reflect the mechanical behavior of the compound resonator. This current-voltage relationship is essentially linear and can be described by the relation $\tilde{i} = \tilde{Y}e_{rt}$, where \tilde{Y} is the admittance, the inverse of the impedance. In the following description, we have borrowed heavily from the formal descriptions given by Tiersten [20].

The stress-strain relation for the overlayer continues to be described by Equation (2), but the stress-strain relation for the quartz takes the form

$$\Pi = c_{66} \frac{\partial u(z,t)}{\partial z} + \eta_{Q} \frac{\partial v(z,t)}{\partial z} + e_{26} \frac{\partial \phi}{\partial z}, \qquad (8)$$

where c_{66} is the mechanical shear modulus for the quartz, $\eta_{\rm Q}$ is the "viscosity" of quartz, e_{26} is the piezoelectric constant appropriate for the AT-cut quartz ($c_{66}=2.901\times 10^{10}~{\rm N/m^2}$, and $e_{26}=-0.095~{\rm C/m^2}$. The quartz "viscosity" is purely an empirical constant and is included to give the unloaded resonator a finite loss. We have found that a value of $\eta_{\rm Q}=0.007~{\rm N\cdot s/m^2}$ yields a theoretical loss for unloaded resonators which approximates the losses in our crystals. In addition to this mechanical stress–strain, the constitutive electrical equation is described by

$$D_2 = e_{2\delta}u(z,t) - \varepsilon_{22} \frac{\partial \phi}{\partial z}, \qquad (9)$$

where D_2 is the electrical displacement in the quartz and ε_{22} is the quartz dielectric constant appropriate to this geometry. This equation specifically couples the mechanical and electrical variables. This set of equations again describe shear waves having the same form as given

in Equation (4), with the difference being that for quartz, the expressions for the propagation constant $k_{\rm Q}$ and the decay constant $\alpha_{\rm Q}$ differ in detail, as shown in the Appendix.

The boundary conditions are the same as those imposed for the mechanical model, and in addition, two electrical boundary conditions are imposed, namely that the potentials at the surfaces of the quartz crystal are given by

$$\phi(0, t) = \phi_0 e^{j\omega t} \tag{10a}$$

and

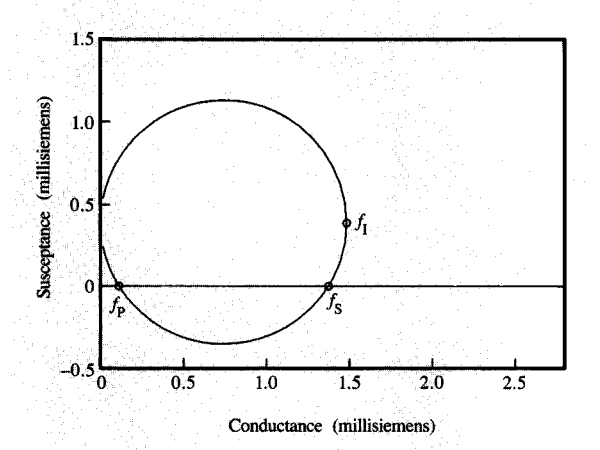
$$\phi(\ell, t) = -\phi_0 e^{j\omega t}. \tag{10b}$$

Detailed means for obtaining the admittance from these equations are presented elsewhere [18] and not reproduced here. However, since an attempt is made here to convey the physical bases of the development, the procedure for calculating the admittance is described. Since the admittance is the current-to-voltage ratio, an expression for the current density must be obtained. Following Tiersten, the current density is taken as the time derivative of the surface charge density, which in turn is the integral of the electric displacement at the surface. For any given frequency ω , the admittance \widetilde{Y} is a complex function of the assumed parameters. We indicate this dependency by writing

$$\widetilde{Y} = \widetilde{Y}(\omega, \rho_0, c_{\epsilon\epsilon}, \eta_0, e_{\gamma\epsilon}, \varepsilon_{\gamma\gamma}, \ell, \rho_1, \mu_1, \eta_1, \varepsilon), \tag{11}$$

where the variables containing the subscript L represent values for the overlayer. The specific relationships that apply are given in the Appendix. This formulation was obtained using a conceptually simple physically based model. We have shown that the earlier study by Benes [17] using equivalent circuit methods yields the identical result when his solution is generalized for a viscoelastic overlayer.

A very useful visual presentation of the information contained in the admittance function is provided by the admittance diagram. The real part of the admittance, the conductance G, is plotted along the abscissa, and the imaginary part, the susceptance B, is plotted along the ordinate. For the sake of illustration, the admittance diagram for frequencies in the neighborhood of the third harmonic resonance of a 5-MHz AT-cut quartz crystal in contact with water is shown in Figure 3. The locus of points traces a circular pattern, traversing in a clockwise fashion with increasing frequency. The effects of the indicated materials parameters on the quartz resonator can be characterized by such an admittance diagram. The frequency f_1 is the "intrinsic" resonant frequency of the resonator. This "intrinsic" frequency is defined as that frequency where the conductance is a maximum. Frequencies at which the admittance is real (where the phase is zero) are of interest, since an ideal electronic



Admittance diagram for the third harmonic resonance of a 5-MHz crystal having one face immersed in water. Frequency increases in the clockwise direction. The three principal resonances are shown and described in the text.

circuit can be designed to oscillate there. These are the "series-resonant" frequency f_s and the "parallel-resonant" frequency $f_{\rm p}$, in analogy with an equivalent electrical circuit. Another characteristic which summarized the resonant behavior is the value of the conductance at f_{t} . This inverse of this conductance is the resistance of the compound resonator at its intrinsic resonance, $R = 1/G_{max}$, and characterizes the losses in the resonator. The quality of the resonance is characterized by the quality factor Q, representing the ratio of the peak energy stored in the energy-storing elements to the energy dissipated per cycle during the resonance. The value of Q is given by the ratio of the resonant frequency to the frequency interval between those frequencies at which the conductance is half its peak value. The radius of the circle is 1/2R. As the losses increase, the radius of the circle decreases.

The ordinate of the center of the circle is not located on the abscissa, but has the same value as the ordinate of the point $f_{\rm I}$. This displacement of the center along the ordinate results from the capacitance between the electrodes of the device and includes not only the dielectric capacitance of the quartz, but also the external wiring and circuit capacitances, $C_{\rm total}$. The ordinate has the value $\omega C_{\rm total}$. The capacitance $C_{\rm total}$ takes on a special significance in the case of lossy overlayers, because as the losses increase, the circle radius is expected to decrease. It is clear that if the losses increase such that R increases toward the value $1/2\omega C_{\rm total}$, $f_{\rm S}$ and $f_{\rm P}$ approach one another; additionally, if R exceeds this value, the circle will no longer intersect the

abscissa. In the case of an oscillating circuit, the phase can no longer attain the null value required for constructive feedback, and oscillations should cease. Thus, the importance of keeping the wiring and circuit capacitances to a minimum when using the resonator with lossy media such as liquids cannot be overstated.

The measured quantities for most experiments are the resonant frequencies and their changes. To quantitate the results with the help of the theoretical calculations, the data must be compared with the appropriate resonance. This section is concluded by demonstrating that results obtained by using the mechanical calculation, while not rigorous, are in excellent quantitative agreement with the intrinsic resonance calculations of the more complete model. To make these comparisons, the frequency from the mechanical model, labeled $f_{\rm M}$, and those from the complete model, f_1 , f_S , and f_P , are determined both for the unloaded resonator and for the resonator loaded with a variety of overlayers. The changes of the resonant frequency $\Delta f_{\rm M}$, $\Delta f_{\rm I}$, $\Delta f_{\rm S}$, and $\Delta f_{\rm R}$ are then calculated and compared. These calculations are computed both for the fundamental resonance and for the third harmonic.

Before examining the results of those calculations, it is instructive to examine two situations which demonstrate that the mechanical resonant frequency $f_{\rm M}$ is most closely related to the parallel resonant frequency f_p . This is perhaps not surprising, since at parallel resonance the admittance is nearly at a minimum, and the current is consequently negligibly small—close to the case for the freely vibrating resonator. For the free mechanical resonances at the fundamental and third harmonic, one would expect exactly a factor of three in the ratio of the frequencies. This is, in fact, true for $f_{\rm M}$ and for $f_{\rm P}.$ In contrast, for f_1 and f_8 , the ratios are 3.00843. Also, for an elastic overlayer, e.g. a $20-\mu m$ -thick layer of copper, the changes $\Delta f_{\rm M}$ and $\Delta f_{\rm P}$ are both found to be -799 610 Hz, while the changes Δf_1 and Δf_2 are found to be -798 010 Hz. The connection between the two sets of resonances is clearly established by these results; the percentage difference in the frequency changes between the two sets is less than a tenth of a percent.

The changes incurred when the overlayer is a thick liquid layer are quite different. The responses to three liquids have been calculated, and the results are tabulated in **Table 1**. The surprising result is that for the case of liquids, $\Delta f_{\rm M}$ mirrors $f_{\rm I}$ rather than $f_{\rm P}$. In the case of mercury, the viscosity is large enough that no series or parallel resonance was expected to exist for the third harmonic. From these calculations, it can be concluded that the mechanical model is quite applicable and that the convenience of its analytical form can be used when only the frequency *change* is of interest.

A shear wave coupled to a liquid has only a finite depth of penetration, limiting the loss of energy into the liquid. This depth is of some interest to electrochemists, since it is useful to compare it with hydrodynamic boundary layers, diffusion layers, electrical double layers, etc. In liquids, the propagation constant and the decay constant have the same value. A depth of penetration δ can be defined by the inverse of the decay constant,

$$\delta = \sqrt{\frac{2\eta_{\rm L}}{\omega\rho_{\rm L}}}.$$
 (12)

For water, this is about 2400 Å at 5 MHz. In mercury, this depth is quite small, about 850 Å. For acetonitrile and dimethyl formamide, it is 1700 and 2400 Å, respectively. Depths can be larger, e.g., 6400 Å for n-hexanol. In general, they are of the order of a few thousands of Å. Changes in the liquid properties within this depth should result in changes in frequency and/or Q. A pictorial representation of a shear wave coupled into water from a 5-MHz resonator is given in **Figure 4**. The normalized displacement is shown as a function of distance into the water at various times, over a half-period interval. The strong predicted damping of the wave amplitude is evident.

Non-electrochemical applications

A feature common to the use of the quartz resonator in the electrochemical environment is the interfacing of the crystal with a liquid or other lossy environment. Before illustrating some electrochemical applications, we describe examples of related studies at the IBM Almaden Research Center on the behavior of the resonator in liquids and other lossy media. During the development of the theoretical descriptions for the resonator behavior, several studies were carried out to find empirical support for the descriptions. Experiments were conducted in the classical manner (that is, with the crystal forming part of an oscillating circuit), and changes recorded in the oscillation frequency. In a group of early studies, one face of the quartz crystal was in contact with a simple liquid [21]. The calculations involved were equivalent to those for the mechanical model with a purely viscous overlayer. The frequency change was related to the density ρ_r and viscosity η_1 of the liquid through the relation

$$\Delta f_{\rm M} = -f_0^{3/2} \sqrt{\frac{\rho_{\rm L} \eta_{\rm L}}{\pi \rho_{\rm O} \mu_{\rm O}}}.$$
 (13)

The system, consisting of a mixture of ethanol and water, provided a stringent test for these calculations, since the $\rho_{\rm L} \eta_{\rm L}$ product for the mixture passes through a maximum in the neighborhood of a 40% ethanol-water mixture. In **Figure 5**, we show a comparison between the calculations using Equation (13) and the measured values, shown as open circles. The frequency of the resonator with pure ethanol was taken as the reference frequency. The agreement was quite good, providing a quantitative

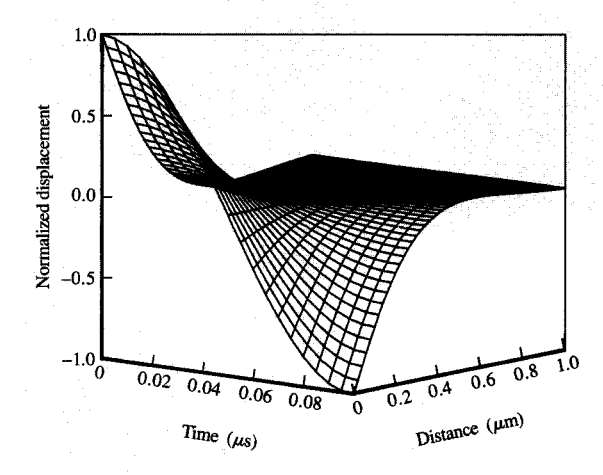


Figure 4

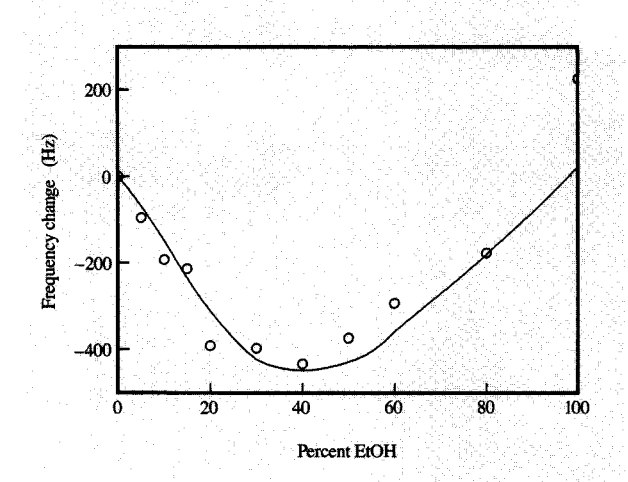
Three-dimensional plot of the predicted propagation of a shear wave into water. The vertical axis represents the normalized displacement, the time axis represents a half period of the wave, and the distance axis represents the distance into the liquid.

Table 1 Comparative changes in resonant frequencies.

Liquid	Harmonic	Δf_{I} (Hz)	$\Delta f_{ m S}$ (Hz)	$\Delta f_{ m P}$ (Hz)	Δf_{M} (Hz)
Water	1	-697	-651	-729	-697
	3	-1206	-942	-1590	-1207
o-nitrotoluene	1	-1285	-1200	-1391	-1285
	3	-2223	-1756	-3759	-2225
Mercury	1	-3290	-2630	-4009	-3288
,	3	-5691	no res.	no res.	-5696

agreement and also reflecting the maximum density viscosity product. Equation (13) was also compared to the behavior of glucose mixtures [22]; the expected monotonic behavior with increasing sugar concentration was found. The frequency shifts for resonators interfaced with liquids have been observed and reported for a large number of solvents by Nomura et al. [23, 24] and by Yao and Zhou [25]. While these shifts are not discussed in any detail here, their observed shifts are found to be consistent with (13), when surface roughness is taken into account.

When the liquid studies were extended to very viscous fluids, such as the perfluoropolyethers, serious discrepancies between the predictions of theory and the observed shifts were noted [18]. For these studies, the crystal was treated as a passive element, and its admittance spectrum was recorded using an impedance



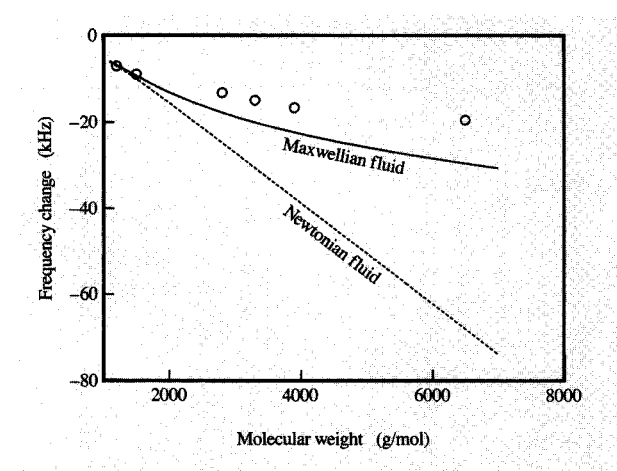
Comparison of observed frequency changes for a water-ethanol mixture (circles) with the quantitative predictions for a Newtonian fluid (solid line).

analyzer. A series of six fluids with molecular weights ranging from 1200 to 6500 g/mol were studied, and the associated frequency changes and resonant resistances were recorded. From the published values for the density and dc viscosity of the fluids, best-fit curves were used to obtain values for the density and viscosity of the fluids as

a function of molecular weight. In this initial treatment, the fluids were considered to be Newtonian; that is, it was assumed that they could be characterized solely by a frequency-independent viscosity. By using these values, theoretical predictions were obtained for the frequency change and resistance of the resonator. The predictions are indicated by dashed lines in **Figures 6** and 7. The empirical data are shown as circles. For both the frequency change and the resistance, the discrepancy is obvious. These discrepancies were resolved by recognizing that at the frequencies used, the fluid exhibits elastic as well as viscous behavior. One model for such behavior is contained in the Maxwell model, in which the viscosity and shear modulus are assumed to be frequency-dependent. For that model,

$$\eta_{\rm L} + j \frac{\mu_{\rm L}}{\omega} = \eta_0 \frac{1}{(1 + j\omega\tau)^{\beta}},\tag{14}$$

where η_0 is the dc viscosity, τ is an empirically determined relaxation time and is related to the molecular weight, and β is an empirical coefficient sometimes interpreted as reflecting a distribution of relaxation times. When the fluid is treated as a viscoelastic Maxwellian fluid, the complete model yields the solutions given by the solid lines in the figures. No protracted effort was made to find a "good" fit. The Maxwellian description modifies the Newtonian description in a manner that brings both the frequency and resistance values much closer to the observed values. The quartz resonator is sensitive to both the viscosity and elasticity of the overlayers, and the predictions of the



Flaure 6

Comparisons of the observed frequency changes for a non-Newtonian fluid (circles) with the quantitative predictions for a Newtonian fluid (dashed line) and Maxwellian fluid (solid line).

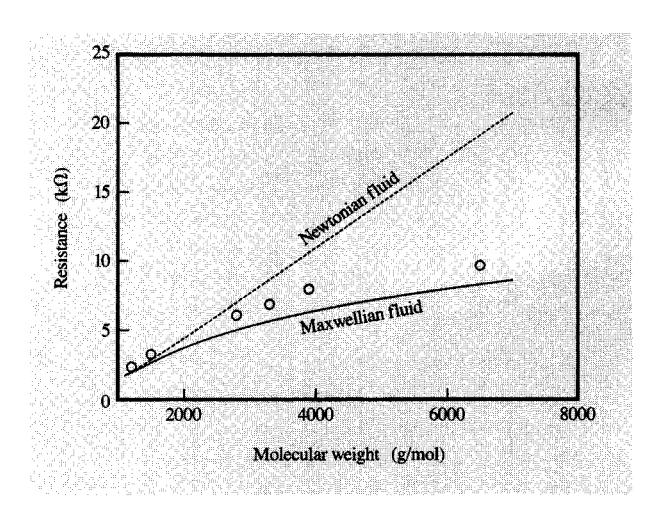


Figure 7

Comparisons of the observed resistance changes for a non-Newtonian fluid (circles) with the quantitative predictions for a Newtonian fluid (dashed line) and Maxwellian fluid (solid line). complete model are in semiquantitative agreement with experiment. It appears that the resonator can fill a role in studies of the viscoelastic properties of thin films, but much more quantitative work must be done in this area.

Another study involved examining the use of the resonator to measure the uptake of solvent into a polymer film coated on its surface. The related study by Moylan et al. [26] reported on the sorption of water in polyimide films. The weight changes were measured both during sorption and desorption. The initial portions of the curves were linear with the square root of time, providing evidence that simple diffusion as described by Fickian processes dominated the process. From the desorption curve, diffusion constants for water in the polyimides studied were found to range from 1×10^{-10} to 5×10^{-9} cm²/s.

In another study, a lithographic polymer film for use in aqueous developers was cast onto the surface of the crystal using a spray-coating technique. The solvent for the polymer was removed by drying the film at 80°C in vacuum. It will be recalled that the acoustic properties of the cast film can be disregarded when the thickness is negligible with respect to the wavelength of the shear wave. To test whether this approximation was appropriate, the thickness of the film was measured with profilometry and compared to the thickness calculated using the thinfilm approximation [Equation (1)], neglecting the acoustic properties of the polymer film. The agreement at a thickness of 3 µm indicated that at least for films of this thickness, the thin-film approximation was appropriate. One face of the crystal was placed in contact with distilled water, and the frequency change was recorded as a function of time. The mass percent change was calculated using (1), and the time dependence obtained is shown in Figure 8. Use was made of a log-log plot in order to distinguish between Type I and Type II diffusions. Type I diffusion is characterized with a $t^{1/2}$ dependence, while Type II diffusion obeys a t dependence. Sorption characterized by values for the exponent of time between 1/2 and 1 is referred to as "anomalous." A linear regression fit neglecting the last four data points yields an uptake proportional to $t^{0.57}$, very close to Type I Fickian behavior.

An example of the sensitivity and accuracy of the quartz resonator in a liquid environment has been provided by Hinsberg et al. [27, 28], who used the resonator to monitor the dissolution of a lithographic polymer. A 1.25-\(mu\)m-thick commercial aqueous-based lithographic polymer was cast onto a 5-MHz resonator and exposed to monochromatic radiation. The resulting interference fringes resulted in a spatially periodic exposure of the polymer, with the regions of constructive interference being highly exposed and the regions of destructive interference only slightly exposed. The polymer was then dissolved in a developer.

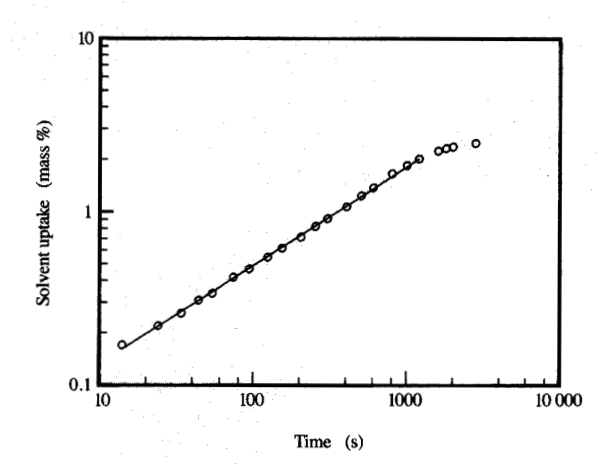


Figure 8

Log-log plot of the observed change in the mass of a lithographic polymer exposed to distilled water. The solid line represents a linear regression to the points and has a slope of 0.57, close to the value of 0.5 characterizing Type I (Fickian) diffusion.

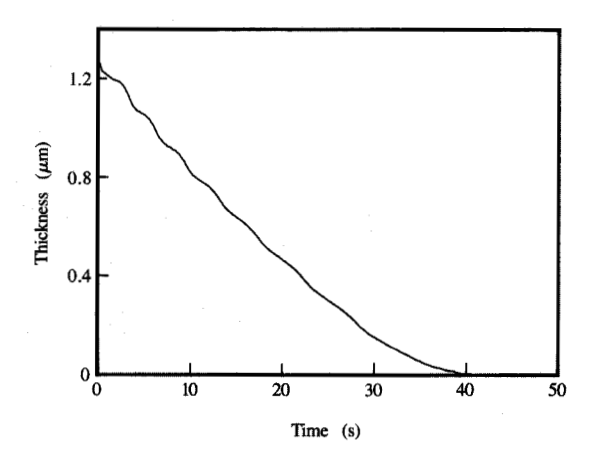
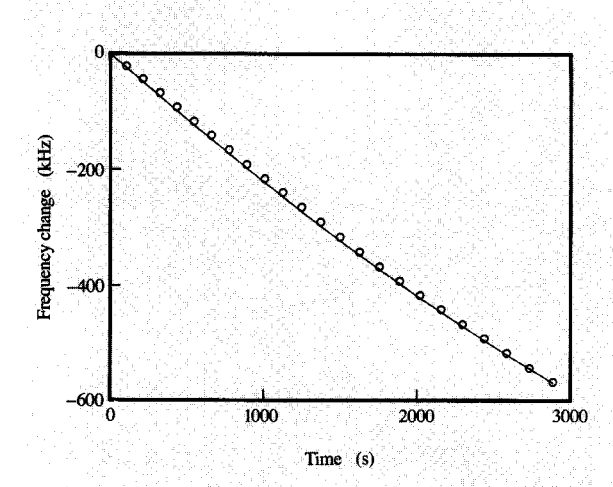


Figure 9

Thickness of a photolithographic polymer film during dissolution after irradiation with monochromatic light. The periodic exposure resulting from the interference of the incident and reflected radiation is evident from the periodic rate of dissolution.

Again by using the linear approximation, the time dependence of the polymer thickness was obtained, as shown in **Figure 9**. The regions of large and small cross-



Observed nonlinear frequency shifts during the galvanostatic deposition of copper from an acid-copper solution, indicated by the circles. The solid line represents predicted frequency changes assuming a 100% Faradaic efficiency.

linking are clearly reflected in the dissolution rate, and the 1300-Å spacing is consistent with the index of refraction of this polymer at the exposure wavelength.

Electrochemical applications

Recently the uses of the quartz resonator as a microbalance in electrochemistry have been reviewed [29]. The focus here is not only on relevant electrochemical investigations taking place at the IBM Almaden Research Center, but also on the development of the technique itself. For electrochemical applications, one of the metal films serving as an electrode for the quartz crystal also serves as the working electrode. During adsorptive/desorptive, deposition/stripping, and oxidation/reduction processes, both the charge and the mass involved in the process can be determined. These two measurements are quite accurate, provided that they are properly decoupled. In principle, the mass per charge of the species involved can be measured. This marks a significant addition to the battery of techniques available to the electrochemist. To ensure that the electrochemical fields and the radio-frequency fields are decoupled, it is necessary that the working electrode be connected to a true ground. The rf fields are thus constrained to be within the quartz, and the electrochemical fields within the electrolyte. For this reason, homemade potentiostats of the Wenking type having the working electrode at true ground are frequently used, although commercial instrumentation can be employed with modification [30].

An additional experimental precaution is needed because of the sensitivity of the quartz crystal on the radial distance from the center of its circular electrodes. Measurements of the radial sensitivity in liquid have recently been reported [31-33], and the same nonuniformity is observed. However, despite this nonuniformity, the relations based on models which assume the use of quartz resonators of infinite lateral extent have been applied successfully to characterize the frequency shifts. To keep the geometry as nearly circular as possible, the electrodes are made asymmetric, with one electrode having a diameter 1.5 times the other. The larger electrode is chosen as the electrochemical working electrode to ensure that the resonator is not sensitive to the edge regions of the working electrode, where current concentration is likely.

In electrochemical applications to date, the quartz resonator has been used to measure mass changes on a surface. Some investigators have determined the mass sensitivity of the microbalance empirically, while others have used the equations developed for vacuum uses, as expressed in the mechanical model. Since mass is the principal quantity of interest, it is appropriate to present some evidence in support of the straightforward use of the theoretical models, without calibration. For these studies, copper was electrolytically deposited onto one face of a quartz microbalance from a solution of 0.5 M H₂SO₄, 0.5 M CuSO · 5H₂O, and 1.1 M EtOH. The deposition was conducted at a constant current of 5 mA on a surface area of 0.39 cm². The uncertainty in the area was 5%. The Faradaic efficiency of acid copper deposition is known to be virtually unity. The frequency change as a function of time is shown in Figure 10, in which the circles represent experimental data points. The time dependence is nonlinear, with the rate of change decreasing with time. At first glance, this may seem surprising, since deposition at constant current should imply a constant rate of deposition; the linear Sauerbrey relation should predict a linear time dependence. The frequency change is well over 10% of the fundamental frequency, indicating a large deposit thickness, where the thickness of the copper is no longer negligible with respect to the wavelength of the shear wave. If the mechanical model is particularized to elastic films, the relatively simple relation first described by Lu and Lewis [8] is obtained, namely

$$\sqrt{\rho_{\rm Q}\mu_{\rm Q}}\tan\left(\omega\ell_{\rm Q}\sqrt{\frac{\rho_{\rm Q}}{\mu_{\rm Q}}}\right) = -\sqrt{\rho_{\rm L}\mu_{\rm L}}\tan\left(\omega\varepsilon\sqrt{\frac{\rho_{\rm L}}{\mu_{\rm L}}}\right). \tag{15}$$

The left-hand side of the equation contains the quartz crystal parameters, while the right-hand side contains overlayer parameters, which include the acoustic shear modulus of the overlayer. Assuming a Faradaic efficiency of 100%, the frequency change resulting from a constant

deposition current of 5 mA can be calculated according to Equation (15), and is shown as the solid line of **Figure 11**. Conversely, the observed frequency changes can be used to calculate the copper thickness ε ; these results are plotted as circles in Figure 11. The thickness increases linearly with time, as anticipated. These results show that even for thick copper films, the mechanical model can be used without a calibrating factor.

Thus, it appears that for thin films, the resonator can function as a microbalance, using the Sauerbrey relation [Equation (1)]. In one of the early applications of the microbalance, Kaufman et al. [34] studied the oxidation and reduction of the conducting polymer, polypyrrole. A quasi-equilibrium technique was employed to apply a stepwise potential to a polymer. After the application of a step of potential, the current was allowed to decrease to below a certain minimum set point before the next step was applied. The charge was obtained by integration of the current, and the mass changes were determined from the observed frequency change. An insulator-to-metal transition was believed to result from the incorporation of anions (ClO_.) during oxidation and their subsequent reversible removal upon reduction. Although a reductive charge was measured during the reduction, surprisingly the mass was observed to increase. This unusual behavior was attributed to the influx of cations (Li⁺) during the reduction. This work illustrated a case for which the application of the microbalance provided dramatic evidence for a result which would not have been anticipated strictly from charge measurements.

Examples of the capability of the electrochemical quartz microbalance as a sensitive device to measure charge-tomass ratios are provided by the studies of monolayer underpotential deposition (UPD) of metals and the adsorption of halogens. In this process, the metal ions in solution are deposited on a foreign metal substrate at potentials anodic of the equilibrium Nernst potential of the depositing metal. The initial UPD work [35] was similar to the earlier work of Bruckenstein and Shay [36]. Whereas Bruckenstein and Shay used 10-MHz resonators, Melroy et al. used the third harmonic of 5-MHz resonators. The use of harmonic modes to increase mass sensitivity was demonstrated. Deakin and Melroy [37] illustrated in a dramatic fashion the accuracy of the microbalance when they predicted the current that would be necessary to account for the observed mass, assuming an electrosorption valency of 2 for the deposition of lead on gold from a perchloric acid solution. That predicted current was compared to the current measured, and the two curves were shown to superpose, as shown in Figure 12. Direct demonstration of the determination of electrosorption valency has been provided by the work of Deakin et al. [38], not only in metal UPD processes, but in the adsorption of bromine and iodine anions as well.

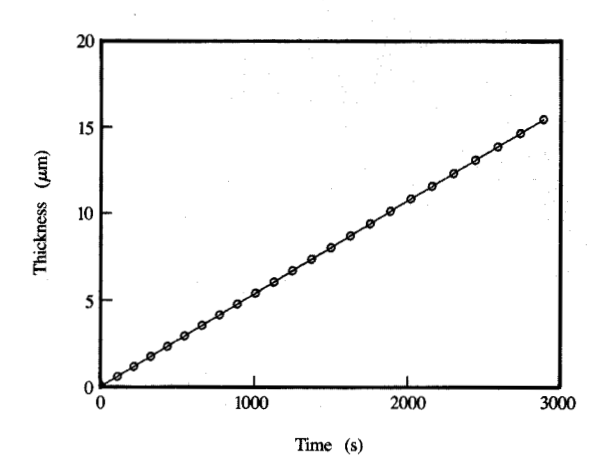


Figure 1

Copper film thickness calculated from the data of Figure 10, using a model that includes the acoustic properties of the copper (circles), compared to predictions based on an assumed 100% Faradaic efficiency (solid line).

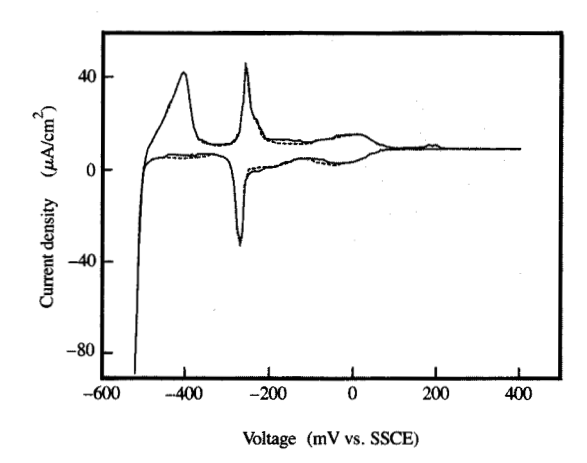
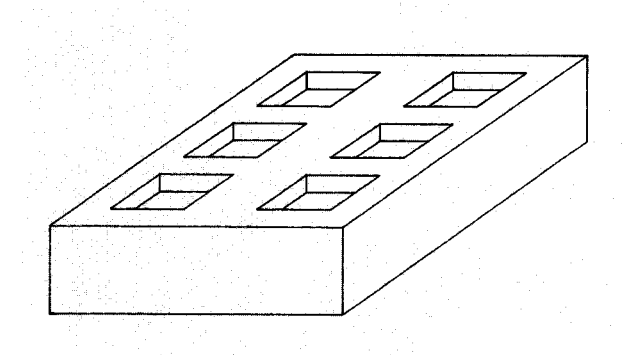


Figure 12

Calculated current density inferred from mass uptake during the underpotential deposition of lead on gold, assuming an electrosorption valency of 2 (solid line), compared with the current density measured during a cyclic scan of potential (dashed line). From [37], adapted with permission.

A different but instructive example of the use of the quartz resonator in electrochemical applications is provided from the evidence for surface reconstruction



Idealized roughened surface, indicating how fluid may be trapped in wells on the surface, causing a frequency shift.

during electrochemical redox cycles [39, 40]. It illustrates the phenomenon of entrapped fluids mentioned in the Introduction. The polycrystalline gold film which served as an electrode in the work also served as the working electrode in an electrochemical cell. The frequency change and the current were recorded as the electrode was oxidized and then reduced in neutral and alkaline solutions. In both cases, the frequency change observed was greater than that expected from the oxidation of the gold. The effect was much more pronounced in the alkaline (NaOH) solution. The additional frequency change was attributed to the entrapment of the solvent in pockets or wells created on the surface during the oxidation. This concept is illustrated in the idealized diagram shown in Figure 13. The wells are idealized as being homogeneous, rectangular, and uniformly distributed. This is highly idealized, of course, but illustrates the concept. Such oxidative roughening was verified directly by scanning electron micrography, and its reversible nature was supported by capacitance studies. The net mass of the trapped fluid can be calculated using the Sauerbrey equation. If the net mass and the density of the fluid are known, an average depth δ can be calculated. Given this roughness, the additional frequency shift due to the entrapped fluid can be expressed by

$$(\delta f)_{\text{ROUGH}} = -\frac{2f_0^2}{\sqrt{\rho_0 \mu_0}} \rho_L \delta. \tag{16}$$

This correction becomes important when $(\delta f)_{\text{ROUGH}}$ is comparable to the frequency change induced by deposition or stripping. In continuous plating applications, although the topography of the deposit can change from that of the smooth gold electrode to some steady-state roughness, the

frequency change induced by the plated metal far exceeds that due to the roughness.

Just as the quartz resonator has served as a deposition monitor for the vacuum industry, it is now also used as a deposition monitor for the electrochemical industry. The impetus toward the development of such an instrument was provided by the application of the quartz resonator as a deposition monitor for electroless NiP deposition [41]. For that purpose, the quartz crystal was placed in a holder of polyvinyl chloride, mounted with an O-ring seal in order to expose only one face to the solution. The oscillator circuitry was placed in this same probe, directly under the crystal. The durability of the crystal, its electrodes, the seals, and the associated electronic circuitry was demonstrated. By using two modified vacuum-deposition rate monitors and the same algorithm for the deposition of the NiP alloy as used for vacuum deposition, 3% agreement was found between the deposition thickness calculated from the frequency change data and that from the average thickness determined using a β -backscattering technique. This not only demonstrated the utility of the quartz resonator as an electrochemical deposition rate monitor, but also demonstrated that the deposition sensitivity is unaffected by immersion in a fluid.

Unanswered questions

The quartz resonator is being successfully applied in an increasing number of ways, placing its behavior in liquid and other lossy media under increasing scrutiny. There have been a number of unresolved issues. The nonuniform sensitivity across the surface has already been mentioned. The evidence is clear that for the basic resonant mode, the sensitivity is bell-shaped across the surface. The shape of this distribution has been measured in vacuum [31, 32] and has recently been determined in a liquid environment [33]. For localized depositions, account must be taken of this variation. Although it is not universally accepted that the theoretical sensitivity [42] can be used for uniform deposition in electrochemical applications, the evidence presented in the examples above indicates that that sensitivity can be used. This area continues to be of substantial interest [43-45].

The no-slip boundary condition which has been assumed in the theoretical treatments has recently come under question. There appears to be evidence that under certain conditions partial slip can occur at the interface [46, 47]. This is a fascinating result which can have important consequences in electrochemical studies when the surface may be such that slippage can occur. An appropriate new boundary condition will have to be determined for the interface and new solutions generated.

From the intuitive understanding of the behavior of the quartz resonator in a liquid, one would expect that changes in the average mass density to a depth of about 1000 Å

should be detectable. Changes in densities of the double layer which extend only to tens or hundreds of Å should be observable. Specifically, the use of an electrolyte asymmetric in cationic and anionic mass should show a variation with potential. In a perchloric acid solution, for example, one would expect a frequency decrease in going from a cathodic bias to an anodic bias. Preliminary experiments have not shown any measurable change. This may be due to the fact that the experimental potentials were not sufficiently close to the potential of zero charge (PZC), the potential at which the net charge on the electrode vanishes.

Frequency changes associated with potential-dependent electroacoustic effects related to the motions induced in the ionic atmosphere in solution have been reported [48]. This would be a very serious additional contribution to the frequency shift; it would have to be understood in order to preserve the quantitative interpretation of frequency shift data. To the authors' knowledge, such an effect has not had to be included in the reduction of electrochemical data. And we have not personally observed effects attributable to such a phenomenon in our electrochemical studies. However, the importance of this possible contribution requires that it be addressed.

The possible behavior of viscoelastic overlayers has been discussed. This area is rich with possibilities, permitting the determination of changes in the acoustic shear properties of such films with changes in their physical and chemical behavior, such as their sol-gel behavior, cross-linking, and the onset of conductivity (in conducting polymer films). The experimental technique needed would require the use of electrical admittance (impedance) methods, an area which is receiving increasing attention [49–52]. From the complete theory, the predicted behavior of the frequency change and the resonant resistance as a function of the thickness of a viscoelastic film are shown in Figure 14. The density was assumed to be 1200 kg/m³, the shear modulus assumed to be 5×10^7 N/m^2 , and the viscosity assumed to be 1.59 $N \cdot s/m^2$. The frequency initially decreases with increasing thickness, but for thickness exceeding 10 μ m, there is a region over which the frequency increases with increasing thickness. The losses associated with the overlayer, as indicated by the resistance, rise rapidly to a maximum near a thickness of 13 μ m. The losses there would be too large to sustain oscillation, but should be measurable using impedance techniques.

Concluding remarks

The efforts at the IBM Almaden Research Laboratory in the application of the quartz resonator to electrochemistry have been quite diverse and have demonstrated its use in a variety of applications. It has been used primarily as a microbalance, using the classical quartz oscillator

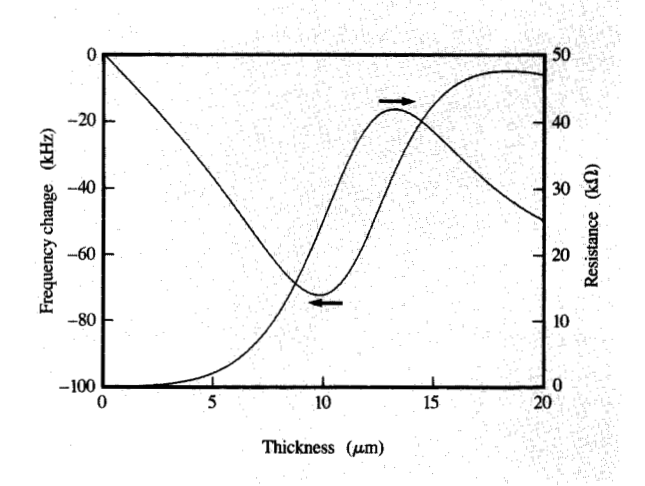


Figure 14

Predicted electrical behavior of a 5-MHz resonator as a function of the thickness of an overlying non-Newtonian viscoelastic film.

technique. A clear understanding of the behavior of the resonator is required for its successful implementation and for an associated analysis of data. Although the use of the mechanical model has been found to be adequate for characterizing resonant frequency changes, use of the complete model in conjunction with admittance measurements may be needed for a more complete characterization-for example, for the characterization of viscoelastic films. The activities described above indicate the major activities of this laboratory in the applications of the quartz resonator. Clearly there exists a large and growing activity in this field in the electrochemical community. As examples of the types of innovative applications being attempted, the work in the use of the quartz resonator as a rotating disk electrode [53] is exciting, and the use of ac gravimetry for kinetic studies [54] is fascinating.

Appendix

Using Equation (3) in Equation (2), the general wave equation for shear waves in a viscoelastic medium is

$$\rho \frac{\partial^2 u}{\partial t^2} = \mu \frac{\partial^2 u}{\partial z^2} + \eta \frac{\partial^3 u}{\partial^2 z \partial t}.$$
 (A1)

In the harmonic approximation, for which solutions are restricted to those having a time dependence of the form $e^{j\omega t}$, the two terms on the right-hand side of Equation (A1) can be combined in terms of a complex viscosity $\tilde{\mu}$, namely $\tilde{\mu} = \mu + j\omega\eta$. The wave equations in (4) are the solutions of the wave equation (A1) in the harmonic

approximation. The values for the associated propagation constant k and the decay constant α are given by

$$k = \omega \sqrt{\frac{\rho}{2(\mu^2 + \omega^2 \eta^2)}} (\sqrt{\mu^2 + \omega^2 \eta^2} + \mu)^{1/2}$$
 (A2)

and

$$\alpha = \omega \sqrt{\frac{\rho}{2(\mu^2 + \omega^2 \eta^2)}} (\sqrt{\mu^2 + \omega^2 \eta^2} - \mu)^{1/2}.$$
 (A3)

If these relations are used in the mechanical model, in the elastic approximation (assuming $\eta_{\rm Q}$ to be zero), it follows that

$$k_{\rm Q} = \omega \sqrt{\frac{\rho_{\rm Q} \mu_{\rm Q}}{2}} \tag{A4}$$

and

$$\alpha_{Q} = 0.$$
 (A5)

Here $\mu_{\rm Q}$ is the "effective stiffened shear modulus" for quartz (the semi-empirical value of 2.947 \times 10¹⁰ N/m² is used).

For the complete model, the wave equation for the quartz differs in detail from Equation (A1). Knowing that there is no free charge in the quartz, Laplace's equation can be written $\partial D_2/\partial z=0$. By using Equation (9), a relation between the displacement u and the potential ϕ can be formulated, namely

$$\frac{\partial^2 \phi}{\partial z^2} = \frac{e_{26}}{\epsilon_{22}} \frac{\partial^2 u}{\partial z^2}.$$
 (A6)

By applying Newton's equations (3) to (8), and using the expression above for $\partial^2 \phi/\partial z^2$, the wave equation for elastic quartz is obtained:

$$\rho \frac{\partial^2 u}{\partial z^2} = \left(c_{66} + \frac{e_{26}^2}{\epsilon_{22}} \right) \frac{\partial u}{\partial z} \,. \tag{A7}$$

In comparing Equation (A1) as applied to lossless quartz with Equation (A7), it is clear that the "effective stiffened shear modulus" $\mu_{\rm Q}$ is replaced by the term $[c_{66} + (e_{26}^2/\epsilon_{22})]$, designated as \bar{c}_{66} . This is the predicted "piezoelectrically stiffened shear modulus" and has a value of $2.924 \times 10^{10} \ {\rm N/m^2}$. This value differs from the semi-empirical value by 0.8%.

The explicit form for the admittance Y can be written as

$$\widetilde{Y} = \frac{i\omega\varepsilon_{22}}{\ell} \frac{N}{D_1 + D_2 - D_3},\tag{A8}$$

where

$$N = k_0 \bar{c}_{66} \sin(k_0 \ell) + k_L \tilde{\mu}_L \tan(k_L \varepsilon) \cos(k_0 \ell_0),$$

$$D_{1} = k_{0}\bar{c}_{66}\sin{(k_{0}\ell)},$$

$$D_{\gamma} = k_{\rm I} \tilde{\mu}_{\rm I} \tan(K_{\rm I} \varepsilon) \cos(k_{\rm O} \ell),$$

and

$$\begin{split} D_{3} &= \frac{2e_{26}^{2}}{\varepsilon_{22}\ell} \left[1 - \cos\left(k_{Q}\ell\right) \right. \\ &\left. + \frac{k_{L}\tilde{\mu}_{L}}{2k_{Q}\tilde{c}_{66}} \tan\left(k_{L}\varepsilon\right) \sin\left(k_{L}\varepsilon\right) \sin\left(k_{Q}\ell\right) \right]. \end{split}$$

Acknowledgments

The authors are indebted to a great number of individuals who have carried out these studies and contributed to them through valuable discussions. Joseph Gordon initiated, supported, and encouraged the development of the technique. Gary Borges has been unfailing in his technical innovation and support. Don Horne's counsel and support in the area of relevant electronics has been indispensable. The path to the complete model, pioneered by Chris Reed and James Kaufman, was essential, and is gratefully acknowledged.

References

- 1. J. C. Brice, Rev. Mod. Phys. 57, 105 (1985).
- 2. G. Sauerbrey, Z. Physik 155, 206 (1959).
- 3. C. Lu, in Applications of Piezoelectric Quartz Crystal Microbalances, C. Lu and A. W. Czanderna, Eds., Elsevier, Amsterdam, 1984.
- 4. K. H. Behrndt, J. Vac. Sci. Technol. 8, 622 (1971).
- 5. C. Lu, J. Vac. Sci. Technol. 12, 578 (1975).
- H. K. Pulker, E. Benes, D. Hammer, and E. Sollner, Thin Solid Films 32, 27 (1976).
- J. G. Miller and D. I. Bolef, J. Appl. Phys. 39, 4589 (1968).
- 8. C. Lu and O. Lewis, J. Appl. Phys. 43, 4385 (1972).
- T. Nomura and O. Hattori, Anal. Chim. Acta 115, 323 (1980).
- T. Nomura and A. Minemura, Nippon Kagaku Kaishi 1980, 1621 (1980).
- T. Nomura, T. Okuhara, and T. Hasegawa, Anal. Chim. Acta 182, 261 (1986).
- T. Nomura and T. Nagamune, Anal. Chim. Acta 155, 231 (1983).
- T. Nomura and M. Iijima, Anal. Chim. Acta 131, 97 (1981).
- P. L. Konash and G. J. Bastiaans, *Anal. Chem.* 52, 1929 (1980).
- W. H. King, Jr., in Vacuum Microbalance Technique, Plenum Press, New York, 1971, p. 183.
- J. Hlavay and G. G. Guilbault, Anal. Chem. 49, 1890 (1972).
- 17. E. Benes, J. Appl. Phys. 56, 608 (1984).
- C. E. Reed, K. K. Kanazawa, and J. F. Kaufman, J. Appl. Phys. 68, 1993 (1990).
- K. K. Kanazawa, in New Characterization Techniques for Thin Polymer Films, H. M. Tong and L. T. Nguyen, Eds., John Wiley & Sons, Inc., New York, 1990.
- 20. H. F. Tiersten, Linear Piezoelectric Plate Vibrations, Plenum Press, New York, 1969.
- K. K. Kanazawa and J. G. Gordon II, Anal. Chim. Acta 175, 99 (1985).
- K. K. Kanazawa and J. G. Gordon II, Anal. Chem. 57, 1770 (1985).
- T. Nomura, M. Okuhara, K. Murata, and O. Hattori, Bunseki Kagaku 30, 417 (1981).
- 24. T. Nomura and M. Okuhara, Anal. Chem. 142, 281 (1982).

- S. Z. Yao and T. A. Zhou, Anal. Chim. Acta 212, 61 (1988).
- C. R. Moylan, M. E. Best, and M. Ree, J. Polym. Sci. 29, 87 (1991).
- W. D. Hinsberg, C. G. Willson, and K. K. Kanazawa, *Proc. SPIE* 539, 6 (1985).
- 28. W. D. Hinsberg, C. G. Willson, and K. K. Kanazawa, J. Electrochem. Soc. 133, 1448 (1986).
- M. R. Deakin and D. A. Buttry, Anal. Chem. 61, 1147A (1989).
- 30. M. D. Ward, J. Phys. Chem. 92, 2049 (1988).
- 31. H. Fukuyo, A. Yokoyame, N. Ooura, and S. Nonaka, Bull. Tokyo Inst. Technol. 72, 1 (1965).
- 32. H. K. Pullar, E. Benes, D. Hammer, and E. Sollner, *Thin Solid Films* 32, 27 (1976).
- M. D. Ward and E. J. Delawski, Anal. Chem. 63, 886 (1991).
- J. H. Kaufman, K. K. Kanazawa, and G. B. Street, *Phys. Rev. Lett.* 53, 2461 (1984).
- O. Melroy, K. Kanazawa, J. G. Gordon II, and D. Buttry, *Langmuir* 2, 697 (1986).
- S. Bruckenstein and M. Shay, J. Electroanal. Chem. 188, 131 (1985).
- 37. M. R. Deakin and O. Melroy, *J. Electroanal. Chem.* 239, 321 (1988).
- M. R. Deakin, T. Li, and O. R. Melroy, J. Electroanal. Chem. 243, 343 (1988).
- R. Schumacher, G. Borges, and K. K. Kanazawa, Surf. Sci. 163, L621 (1985).
- R. Schumacher, J. G. Gordon, and O. Melroy, J. Electroanal. Chem. 216, 127 (1987).
- K. K. Kanazawa and S. K. Doss, *Plating & Surf. Fin.* 74, 52 (1987).
- 42. Hitoshi Sekimoto, *IEEE Trans. Sonics & Ultrasonics* SU-31, 664 (1984).
- D. M. Ullevig, J. E. Evans, and M. Grant Albrecht, *Anal. Chem.* 54, 2341 (1982).
- L. Wimmer, S. Hertl, J. Hemetsberger, and E. Benes, Rev. Sci. Instrum. 55, 605 (1984).
- C. Gabrielli, M. Keddam, and R. Torresi, J. Electrochem. Soc. 138, 2657 (1991).
- E. T. Watts, J. Krim, and A. Widom, Phys. Rev. 41, 3466 (1990).
- M. Thompson, C. L. Arthur, and G. K. Dhaliwal, *Anal. Chem.* 58, 1206 (1986).
- F. Josse, Z. A. Shana, D. E. Radtke, and D. T. Haworth, IEEE Trans. Ultrasonics 37, 359 (1990).
- 49. M. Schmid, E. Benes, and R. Sedlaczek, *Meas. Sci. & Technol.* 1, 970 (1990).
- R. Beck, U. Pitterman, and K. G. Weil, *Ber. Bunsenges. Phys. Chem.* 92, 1363 (1988).
- 51. F. Egger and Th. Funck, *J. Phys. E: Sci. Instrum.* **20**, 523
- H. Muramatsu, E. Tamiya, and I. Karube, *Anal. Chem.* 60, 2142 (1988).
- A. Grzegorzewski and K. E. Heuser, J. Electroanal. Chem. 228, 455 (1987).
- 54. S. Bourkane, C. Gabrielli, and M. Keddam, J. Electroanal. Chem. 256, 471 (1988).

Received January 21, 1992; accepted for publication September 16, 1992

Kay Keiji Kanazawa IBM Research Division, Almaden Research Center, 650 Harry Road, San Jose, California 95120 (KANAZAWA at ALMADEN, kanazawa@almaden.ibm.com). Dr. Kanazawa received a B.S. in physics from the University of California at Los Angeles in 1958, and a Ph.D. in solid state physics from the University of Illinois in 1964. He joined the IBM Research Division at San Jose in 1968 from the faculty of the University of California at Riverside to study photoconductive and dielectric films. His present interests center around interfacial behavior, including electrical, chemical, and hydrodynamic phenomena. Dr. Kanazawa is a member of the American Chemical Society, the American Physical Society, and The Electrochemical Society.

Owen R. Melroy IBM Research Division, Almaden Research Center, 650 Harry Road, San Jose, California 95120 (MELROY at ALMADEN, melroy@almaden.ibm.com). Dr. Melroy received a B.S. in chemistry and a B.A. in mathematics from the University of Tennessee in 1978, and a Ph.D. in analytical chemistry from the University of North Carolina in 1982. He then joined the IBM Research Division in San Jose, where he pursued mechanistic studies of electroless metal deposition. His current interests center on the use of X-ray techniques such as extended X-ray absorption fine structure (EXAFS) and X-ray scattering—and the use of electrochemical quartz microbalance—to probe the structure of electrochemical interfaces. Dr. Melroy is a member of The Electrochemical Society.

